

ANALYSIS OF SLIP FACTORS IN CFD CALCULATIONS – ASSESSMENT OF LITERATURE MODELS

*M. Waesker*¹, T. Goetz*, B. Buelten*, N. Kienzle**

*Fraunhofer Institute for Environmental, Safety, and Energy Technology UMSICHT, 45046
Oberhausen, Germany, ¹markus.waesker@umsicht.fraunhofer.de

ABSTRACT

Several slip models like the Stodola, Pfleiderer, Wiesner as well as Qiu model are published in the literature. All of them are semi-empirical models considering the flow phenomena, which lead to outlet flow deviation. In this paper, a CFD-based DOE with 598 centrifugal compressor impellers and a large variation in compressor design parameters is calculated for assessing the literature models. In a first step, an automated simulation workflow for centrifugal compressor impellers is described in detail. Overall, seven geometrical parameters as well as the mass flow and rotational speed are analyzed. The CFD setup is validated based on the Eckardt publication with focus on the slip factor. A DOE based statistical ranking underlines that the Wiesner model suits best to the CFD data. Finally, the main influences on the compressor slip are determined in an analysis of variance. These are the specific speed, blade number, blade outlet angle as well as turning rate.

KEYWORDS

**CENTRIFUGAL COMPRESSOR, SLIP MODELLING, SENSITIVITY ANALYSIS,
NUMERICAL FLOW SIMULATION**

NOMENCLATURE

b_2	Exit blade height	[m]
c_{m2}	Meridional velocity in absolute system (impeller exit)	[m/s]
c_{u2}	Circumferential velocity in absolute system (impeller exit)	[m/s]
$c_{u2\infty}$	Ideal impeller exit circumferential velocity	[m/s]
d_1	Impeller inlet mean diameter	[m]
d_2	Impeller outlet diameter	[m]
F	Shape factor (Qiu model)	[-]
h	Relative blade shroud clearance gap	[-]
m	Meridional blade length	[m]
\dot{m}	Mass flow	[kg/s]
N	Rotational speed	[U/min]
n_s	Specific speed	[-]
P	Empirical diffuser parameter (Pfleiderer model)	[-]
p_{t0}	Total inlet pressure	[bar]
Q_0	Compressor inlet volume flow	[m ³ /s]
r_1	Impeller inlet mean radius	[m]
r_2	Impeller tip radius	[m]
R	Evaluation radius	[m]
t	Blade thickness	[m]
T_{t0}	Total inlet temperature	[K]
s_2	Pitch length at impeller exit	[m]
u_2	Impeller tip speed	[m/s]

y	Specific compressor work	[kJ/kg]
y^+	Normalized near wall distance	[-]
Z	Blade number	[-]
$\beta_{2,\infty}$	Blade outlet metal angle (towards radial direction)	[°]
γ_2	Meridional inclination angle	[°]
$(d\beta_{\infty}/dm)_2$	Meridional blade outlet turning rate	[°/m]
Δh_{is}	Isentropic enthalpy rise	[kJ/kg]
$\Delta\mu$	Slip factor difference	[-]
ε_{Limit}	Diameter ratio limit (Wiesner model)	[-]
θ	Blade outlet rake angle	[°]
μ	Slip factor	[-]
μ_{CFD}	CFD-based slip factor	[-]
μ_{Model}	Literature-model-based slip factor	[-]
ρ_2	Density at impeller exit	[kg/m ³]
Φ_2	Flow coefficient	[-]
ψ'	Empirical factor based on $\beta_{2,\infty}$ (Pfleiderer model)	[-]

1 INTRODUCTION

The turbomachinery demand is shifting to small and flexible units. Especially in the field of centrifugal compressors, innovative applications with new and challenging requirements are developed. Turbomachinery design engineers face the task of designing this new turbomachinery targeting usual low costs and high efficiencies.

To achieve efficient and low cost turbomachinery, the design process has to be accurate and fast. Therefore, researchers have to focus on the 1D modelling of turbomachinery in the early design steps. In the field of centrifugal compressors, emphasis is placed on slip modelling. The slip in compressors is the deviation in the flow angle from the impeller blade outlet angle. Due to slip, the possible compressor power and pressure rise is lowered. An accurate estimation of compressor slip is therefore crucial in the early design phase.

There are several slip models based on qualitative assumptions or empirical factors, which are calculated from literature compressor tests. Stodola published one of the first models in 1924, which depends on the potential theory. Pfleiderer and Petermann (1996) extended the models based on the potential theory with viscosity effects in 1952. The semi-empirical model of Wiesner (1967) is one of the most used slip model. Qiu (2011) published a slip model applicable to both, axial and centrifugal compressors.

The difficulty of all of the mentioned models is the lack in high-fidelity data for evaluation and model creation. All of them are based on pump or centrifugal compressor hardware test data. Therefore, a stepwise parameter variation as well as a conceptualized sampling plan is not possible as it is too expensive. Computational fluid dynamic (CFD) simulations enable huge variation ranges as well as a sampling plan. There are different studies on slip factors in CFD simulations:

In the study of Guo and Kim (2004), an improved slip factor model for forward-curved centrifugal fans is developed. For this, one forward-curved fan is analyzed for different operating points. The numerical simulations were both, steady and unsteady and the k- ε -model is chosen as turbulence model. Different literature models are compared to the mass flow averaged and area averaged circumferential velocity at impeller outlet in the CFD. The authors detected a decreasing slip factor with increasing flow coefficient. Based on the results, a slip model correction for the impeller blockage is introduced.

Huang et al. (2013) investigated the influence of the blade number, the specific speed, the blade wrap angle as well as blade outlet angle on the slip factor. For these four parameters, a design of experiments (DOE) including eight impellers is analyzed and five different mass flow rates are computed. For all impellers, the slip is increasing with increasing normalized mass flow rate. The

influence of specific speed is low compared to the influence of blade outlet angle, blade number and blade wrap angle. The slip factors are in the range of 0.86 and 0.92.

Stuart et al. (2018) analyzed the CFD as well as gas stand test data of six automotive turbocharger compressors. Based on this data, a three-zone slip model is introduced. For this, the authors separate the impeller exit flow into a jet, wake and recirculation region. Individual compressor slip considerations for each region lead to a significant drop of slip factor error. Furthermore, a huge influence of the operating point on the slip factor was detected.

Harrison and Ley (2020) introduced a slip modelling approach based on non-dimensional parameters. For this, the tip speed Mach number, loading coefficient as well as flow coefficient are considered. The method is proven for the CFD data of five different literature compressor stages. The influence of the operating point on the compressor slip is considered in the model and the accuracy is high.

In contrast to the reviewed publications, the focus of this paper is on the assessment of published literature slip models. Therefore, a method for automatic centrifugal compressor flow simulation is introduced and the CFD-setup is validated. In addition, a DOE is calculated and the data forms the basis for the assessment of the slip models. This enables a statistical ranking of the known slip models.

2 METHODOLOGY AND VALIDATION OF CFD SETUP

On the one hand, CFD simulations offer a cheap determination of the centrifugal compressor performance compared to test bench measurements. On the other hand, the modelling and computation leads to errors like discretization or convergence errors and therefore CFD simulations tend to overpredict both, the pressure ratio and efficiencies. Nevertheless, a thorough parameter variation is possible. In the following, a workflow for parameterized centrifugal compressor impeller calculation is introduced. In this workflow both, CFD simulations as well as literature models are taken for the calculations. Furthermore, the geometry creation of centrifugal compressor impellers and the validation of CFD simulation setup is described.

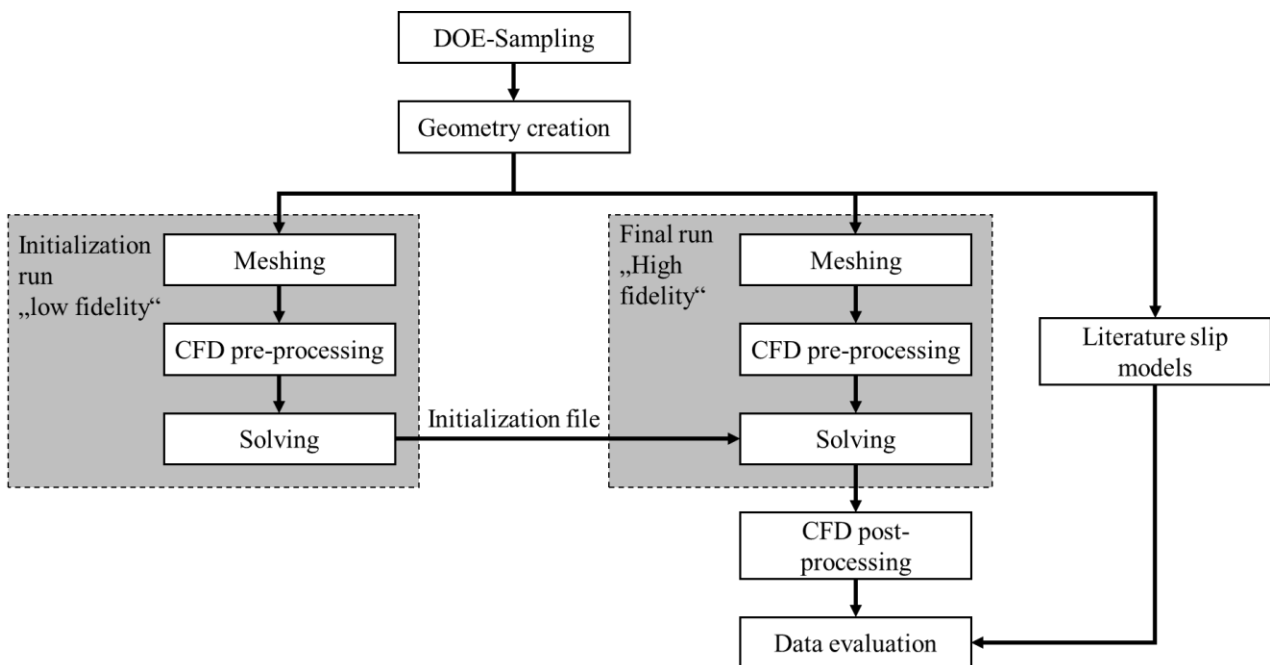


Figure 1: Scheme of the workflow for compressor slip calculation

Workflow for compressor slip calculation

The workflow further developed and used in this work is essentially based on the workflow presented by Kienzle et al. (2019). In that publication, the authors introduced a coupling of geometry creation, meshing, preprocessing and solving for automatic CFD-calculations. The automation is programmed in the software ANSYS OptiSLang[®]. In figure 1, this automation is shown in the grey

box. In this study, the workflow is further developed: A method for geometry creation of centrifugal compressor impellers is developed, the robustness is enlarged by an initialization run and the calculation of literature slip models is integrated.

For the geometry creation, two different modules of ANSYS Workbench are used: Vista CCD and BladeGen. Vista CCD enables the definition of the hub and shroud contour as well as blade angles based on general compressor parameters. These parameters are defined in the following chapter. The defined contours and angles of Vista CCD are processed to BladeGen to achieve Bezier curves for the hub, shroud and blade contour. BladeGen is coupled to the meshing of the CFD runs.

Due to the large range of varied geometry parameters, the automated simulation workflow is divided into two sections. In the initialization section, a coarse “low fidelity” mesh is applied to the geometry. Therefore, a result without a pre-defined initialization file is calculated with low computational effort. That result file is used as the initialization file for the second section, where a “high fidelity” fine mesh is applied to the same geometry. The dependency between the two CFD runs is shown in figure 1. In the studies for this paper it turns out that this combination of “low fidelity” and “high fidelity” CFD-runs is faster and more robust than a non-initialized “high fidelity” CFD run.

For the calculation of literature slip models, the different models are implemented into a calculation environment in ANSYS OptiSLang[®]. The geometry creation module provides the input parameters for the calculation. The determined slip factors are linked to the data evaluation module. In this module, the literature slip factors and CFD slip factors are compared.

Validation of CFD simulation setup

For the validation of the CFD simulation setup, the Eckardt impellers RotorA and Rotor0 are used. Eckardt (1980) analyzed the influence of impeller back-sweep for two geometrically comparable unshrouded compressors with different back sweep angles (Rotor0: $\beta_{2,\infty}=0^\circ$; RotorA: $\beta_{2,\infty}=-30^\circ$). For the analyses, a laser to focus velocimeter (L2F) measurement was applied. Hence, detailed flow measurements and analyses are enabled with the L2F technique. The geometry is published (Schuster and Schmidt-Eisenlohr, 1980) and the different velocity profiles and slip factors are well documented (Eckardt, 1980).

In general, the slip factor enables the determination of fluidic power difference between ideal and real impeller outflow conditions. For swirl free inlet flow, the real circumferential outflow velocity c_{u2} is compared to an ideal circumferential velocity $c_{u2\infty}$. In this case, the ideal outflow velocity is the velocity conform to the impeller blade angle $\beta_{2,\infty}$. In equation 1, this dependency on the blade angle, impeller tip speed as well as meridional outflow velocity c_{m2} is given (Braembussche, 2019). In this paper, the European definition of the slip factor (based on $c_{u2\infty}$) is used. In the American definition, the impeller tip speed u_2 is used as the divisor. Therefore, the results of this paper might differ slightly to the results with the American definition. Furthermore, all angles in this paper are defined towards the radial direction.

$$\mu = \frac{c_{u2}}{c_{u2\infty}} = \frac{c_{u2}}{u_2 - c_{m2} \cdot \tan\beta_{2,\infty}} \quad (1)$$

For the CFD calculations, ANSYS[®] CFX 19.0 is used. As boundary conditions, the total inlet pressure and total temperature as well as the outlet mass flow is set. Furthermore, the rotational speed is fixed. The solid boundaries are defined as adiabatic in addition, with the no slip wall condition. For the fluid modelling, the air ideal gas model is utilized. The change between rotating and stationary domains is simulated using the mixing plane model with constant total pressure. The turbulence is modelled using the shear stress transport (SST) model with y^+ -values around 1.0. The mesh is a structured mesh with hexahedrons. Furthermore, the viscous work term is included for energy equation modelling. As convergence criteria, the relative root mean square error of outlet velocity and

inlet Mach number has to be lower than 0.1 % in the interval of fifty iteration steps. Furthermore, the RMS residual convergence criteria is $1e^{-5}$.

As shown in equation 1, the slip factor depends on the velocity components at the impeller exit. The “jet-wake” velocity profile close to the outlet region of the impeller leads to difficulties in the determination of velocity components for both, CFD calculations as well as L2F measurements (Eckardt, 1975, 1980). Due to this reason, Eckardt measured the meridional velocity component at $R=1.017*r_2$ (Eckardt, 1975). For the circumferential velocity, two different possibilities exist: The determination with the compressor power and Euler equation (chosen by Eckardt) or with circumferential averaging of the velocity components. In this paper, the averaging of the velocity components is used to ensure equal evaluation positions for both velocity components. This method is also chosen in the papers of Huang et al. (2013) as well as Guo and Kim (2004). For the averaging of the different thermodynamic and aerodynamic values the publication of Cumpsty (1989) is used. Hence, the static pressure as well as meridional velocity component is determined based on the area averaging. For all other values, the mass flow averaging is used. For all impeller simulations, the measurement position of Eckardt ($1.017*r_2$) is applied. This measurement plane as well as the outlet, inlet and mixing plane are visualized in figure 2. In this figure, no diffuser domain is visualized. For the validation of the Eckardt data, the vaneless diffuser of the test bench is integrated. In contrast, no diffuser is considered for the DOE impeller simulations in chapter 3. In the following comparison of the CFD simulations to measurement data, the focus is on the correct simulation setup and evaluation procedure. Especially, the measurement position ($1.017*r_2$) is checked.

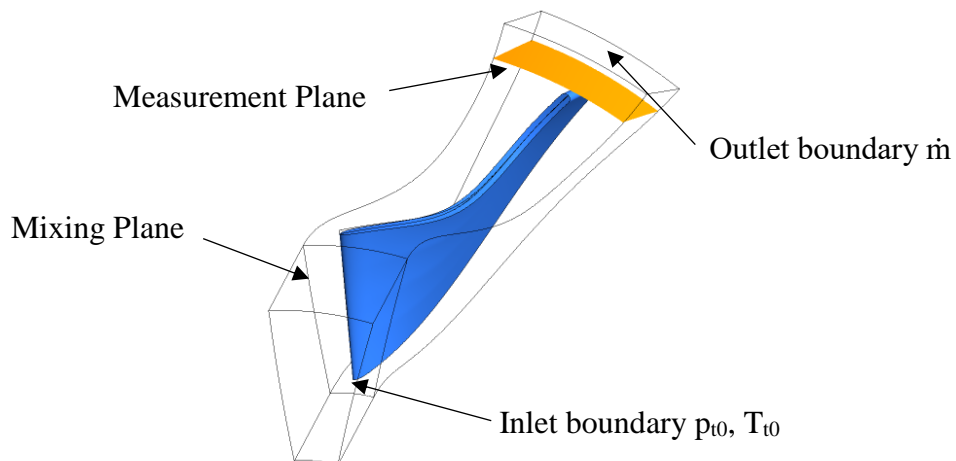


Figure 2: Visualization of the CFD fluid domain with frame change and boundary conditions

For the Eckardt impeller Rotor0 a mesh independence study is conducted. For comparison reasons, the grid convergence index (GCI) is calculated based on the publication of Roache (1994). The GCI enables a comparable quantification of the uncertainty due to grid refinement (for more information see (Roache, 1994)). The mesh size influence is analyzed based on the pressure ratio. Overall, five different meshes are calculated with sizes between 1.8 and 5.5 million nodes. The GCI drops from 1.12 % to 0.187 % for the finest mesh. As a trade-off between accuracy and limited computational power, the second finest mesh with 4.13 million nodes and a GCI of 0.519 % is chosen. The focus of the studies, the slip factor, has a maximum variation of 0.2 % in the five meshes.

In figure 3, the measurements and CFD results are compared for a variation in rotational speed and mass flow. For both, the CFD simulation and L2F measurements, the influence of rotational speed is low. The CFD Results of Rotor0 ($\beta_{2,\infty}=0^\circ$) are in very good agreement to the L2F measurements. The numeric results for RotorA ($\beta_{2,\infty}=-30^\circ$) show slightly higher slip factors compared to the measurements. The error is still in an acceptable range with a mean relative error of 1.0 %. Huang et al. (2013) detect similar differences for their comparison of CFD- to measurement- data of RotorA.

Overall, the CFD results show a high concordance with the L2F measurements. More importantly, the influence of mass flow and rotational speed is similar for both methods.

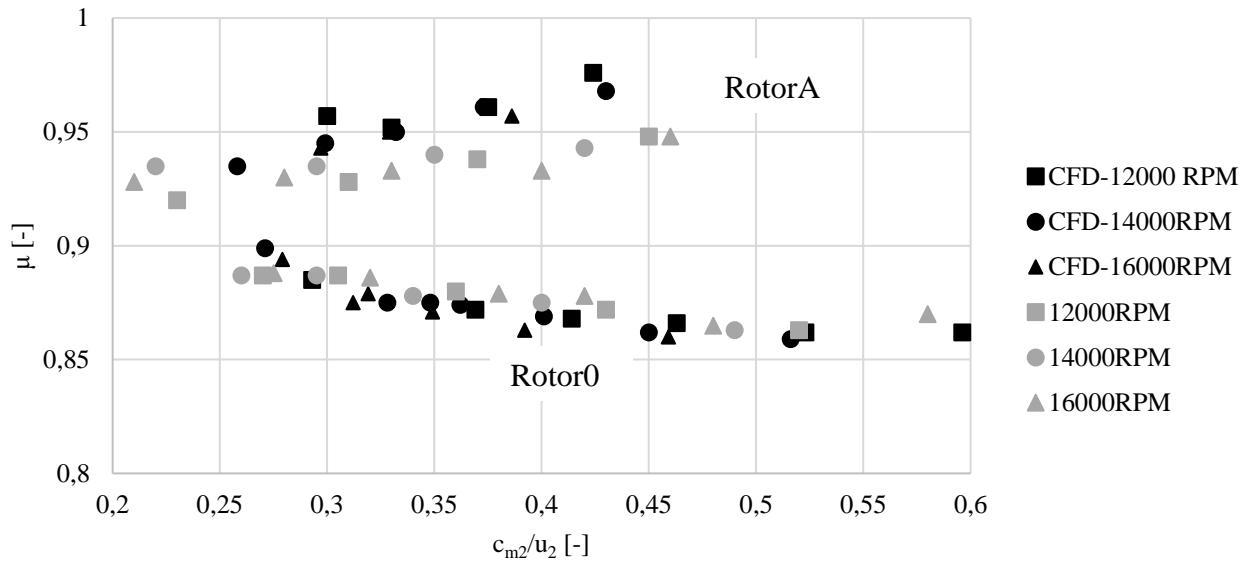


Figure 3: Validation of the CFD simulation (black) for the data of Eckardt (1980) (grey)

3 REVIEW OF LITERATURE MODELS AND CFD-BASED SENSITIVITY ANALYSIS

In the following chapter, a CFD-based sensitivity analysis of literature slip models is conducted. In a first step, the theoretical influences of different parameters on the compressor slip are analyzed. Afterwards, four well-known slip models are summarized. In addition, the model parameters as well as physical assumptions are stated. These models are examined based on a DOE in the end of the chapter.

Theoretical influence of impeller parameters on compressor slip

The compressor slip is a non-viscous and two-dimensional phenomenon. It can be explained with the relative channel vortex model. Due to the rotation of the impeller, the radial fluid flow is redirected in circumferential direction because of the centrifugal forces. This results in a speed and pressure gradient between the pressure and suction side. The gradient induces the relative channel vortex. The vortex causes a deflection of the fluid flow at the outlet (Bräunling, 2009). Viscous and three-dimensional flow effects like the Coriolis vortex and other secondary flow phenomena reinforce this slip phenomenon. Furthermore, low kinetic energy fluid near the suction side changes the flow angle. This phenomenon is described in the jet wake model. The wake-region is caused by secondary flow transporting low kinetic energy fluid to the suction side. Hence, this jet-wake-area leads to flow deflection (Eckert and Schnell, 1961). In addition, the boundary layer and thus velocity gradients impact on the compressor flow (Braembussche, 2019). Therefore, the slip factor in equation 1 is just a model to quantify the influence of the described flow phenomena on the impeller flow and reduced compressor power.

Besides aerodynamic influences, the impeller geometry affects the secondary flow and thus the slip factor. It turns out that the number of blades has the greatest influence on the reduced performance. A high number of blades means an almost blade-compliant flow guidance leading to a small reduction in deflection (Eckert and Schnell, 1961). If the blade curves backwards, the flow separation on the blade suction side decreases, since the relative flow is decelerated over a longer distance with the same pressure ratio (Cumpsty, 1989). A positive wake angle leads to a shift of the suction-side flow separation in the direction of the rear edge, or to the complete suppression of the phenomenon (Braembussche, 2019). The gap height has a direct influence on the gap flow. This causes fluid to flow from the pressure side to the suction side and blocks the channel in the form of a

split vortex (Braembussche, 2019). The blade wake is influenced by the blade trailing edge thickness. Within the wake, there is a significant reduction in speed, which leads to an increased deflection of the absolute speed (Eckert and Schnell, 1961). The diameter ratio d_2/d_1 influences the type of pressure generation and profile shape. Hence, the Coriolis vortex and other secondary flow phenomena are influenced.

Review of literature slip models

The models of Stodola, Pfleiderer, Wiesner and Qiu are among the established slip literature models of the last 100 years. These models differ in their assumptions and considerations and will be briefly introduced with a formula in the following. If the authors used the American slip definition, the formulation is transformed to the European definition for comparison reasons (Bräunling, 2009).

Stodola (1924) considers an average value for the change of the circumferential component of the relative velocity resulting from the angular velocity and the passage width. Here, the superposition of the relative velocity with the relative passage vortex is used to linearly approximate the velocity distribution perpendicular to the flow direction. The number of blades and the blade trailing edge angle in formula 2 show these assumptions. In addition, the flow coefficient can be considered as an important factor influencing the flow velocity in the blade passage.

$$\mu = 1 - \frac{\pi \cos\beta_2}{Z \cdot 1 + \phi_2 \cdot \tan\beta_{2,\infty}} \quad (2)$$

Pfleiderer and Petermann (1996) developed a simple method that can be used for almost all applications (First edition of the book from 1952). The compressor slip is considered the difference between ideal work transferred from blade to fluid and real work, whereby the real work is reduced by the slip factor (work reduction factor). This method assumes a constant blade loading over the blade height. The main parameters included in the slip factor in equation 3 are the number of blades as well as the diameter ratio r_1/r_2 . Furthermore, the trailing edge angle of the blades and the type of diffuser are taken into account by using an empirical factor P.

$$\mu = \frac{c_{u2}}{c_{u2\infty}} = \left(1 + \frac{2\psi'}{Z \cdot \left(1 - \left(\frac{r_1}{r_2} \right)^2 \right)} \right)^{-1} = \left(1 + \frac{2P \cdot (1 + \beta_{2,\infty}/60)}{Z \cdot \left(1 - \left(\frac{r_1}{r_2} \right)^2 \right)} \right)^{-1} \quad (3)$$

Wiesner (1967) developed a model mainly based on empirical results. It determines the circumferential component of the absolute velocity by approximation, taking into account the number of blades, the flow coefficient and the blade trailing edge angle (equation 4).

$$\mu = \frac{c_{u2}}{c_{u2\infty}} = 1 - \frac{\pi}{Z^{0,7}} \cdot \left[1 - \left(\frac{\frac{r_1}{r_2} - \epsilon_{limit}}{1 - \epsilon_{limit}} \right)^3 \right] \cdot \frac{\sqrt{\cos\beta_{2,\infty}}}{1 + \phi_2 \tan\beta_{2,\infty}} \quad (4)$$

Qiu (2011) divides the circumferential component of the absolute velocity into a radial, a curvature and a passage component and thus enables the determination of the slip factor for axial, radial and diagonal compressors (equation 5). For a radial machine, the radial component and the blade curvature has the largest influence, while the passage component can be neglected due to its small effect. The reduced capacity factor is finally derived by considering a form factor F for the different compressor types, the number of blades, the blade trailing edge angle and the flow coefficient.

$$\mu = 1 - F \cdot \left[\frac{\pi \cos \beta_{2,\infty} \sin \gamma_2}{Z} + \frac{s_2 \phi_2}{4 \cos \beta_{2,\infty}} \left(\frac{d\beta}{dm} \right)_2 - \frac{\phi_2 s_2 \sin \beta_{2,\infty}}{4 \rho_2 b_2} \left(\frac{d\rho b}{dm} \right)_2 \right] \cdot \frac{1}{1 + \phi_2 \tan \beta_{2,\infty}} \quad (5)$$

Conducted CFD-based sensitivity analysis

In the review of literature slip models, the different influences of the parameters are examined. As a summary, the different parameters are compared in the upper part of table 1. The blade number Z and impeller exit blade angle $\beta_{2,\infty}$ are included in all models. In addition, Qiu et al. (2011) take the blade turning rate $(d\beta_{\infty}/dm)_2$ as well as the pitch length at impeller exit s_2 into account. Pfleiderer and Petermann (1996) include the diameter ratio in their model. Wiesner (1967) also includes this ratio for diameter ratios exceeding a certain limit.

For the assessment in this paper, nine parameters are varied. The bottom part of table 1 contains the ranges of those parameters. Not all eleven parameters can be varied individually, as they are not independent. Therefore, the blade turning rate $(d\beta_{\infty}/dm)_2$ as well as pitch length at impeller exit s_2 are not included in the DOE. In addition, a parametrization of the blade turning rate would lead to frequent failures in the geometry design process. Nevertheless, there is an intrinsic variation of blade turning rate and passage width due to the dependence on other parameters.

Table 1: Summary of the parameter influence in literature slip models as well as parameters analyzed in CFD-study giving their ranges; ~ means indirectly varied in CFD assessment

	Z	$\beta_{2,\infty}$	d_2/d_1	$(d\beta_{\infty}/dm)_2$	s_2	d_2	θ	h	\dot{m}	t	N
Stodola	x	x									
Pfleiderer	x	x	x								
Wiesner	x	x	x								
Qiu	x	x		x	x						
Unit	[-]	[°]	[-]	~	~	[m]	[°]	[-]	[kg/s]	[mm]	[U/min]
Min	10	-60	1.6			0.2	0	0.95	1.5	1	3,000
Max	30	0	3.3			0.7	30	0.995	4.0	4	35,000

A DOE with 1500 sample points is conducted. For this, a latin hypercube sampling is used. The latin hypercube sampling is well-suited for turbomachinery samplings as reviewed by Waesker et al. (2020). As stated in this paper, a sample size of 50 times the number of parameters should be targeted. Since nine parameters are analyzed in this study, at least 450 succeeded designs are needed. Due to failures in the geometry creation process, the meshing initialization process as well as missing convergence, only 598 out of 1500 designs are taken for the assessment. Nevertheless, the DOE is analyzed based on the probability density function and it becomes apparent that the DOE is still sufficient homogenous. Furthermore, the targeted sample size is reached. The total pressure ratios of the 598 impellers are between 1.5 and 4.5. The isentropic impeller efficiencies are between 79.2 % and 95.4 %. The Reynolds numbers based on the blade exit height are between $1 \cdot 10^5$ and $8 \cdot 10^5$. Especially the compressors with high pressure ratios and low efficiencies are exposed to strong secondary flows and boundary layers. The slip models might get problems with these flow phenomena, but as all models are compared to the same data base, the comparison is still applicable and assimilable.

For the assessment, three statistical values are used. For this, the absolute difference $\Delta\mu$ between the slip factor in the literature model μ_{Model} and the CFD simulation μ_{CFD} is examined for all 598 converged designs individually (equation 6). For the comparison, the maximum and mean value of this difference $\Delta\mu$ is computed for all DOE sample points. Furthermore, the root mean square error (RMSE) of the slip factor is examined based on the 598 compressor impeller simulations.

$$\Delta\mu = \mu_{Model} - \mu_{CFD} \quad (6)$$

Table 2 shows the results for the mentioned statistical values for all four models. The maximum difference is significantly higher in the Stodola model compared to the other three models (around 30 % higher). The mean difference between the models and CFD simulation is also the highest for the Stodola model. In this case, the Wiesner model shows the highest agreement to the CFD results. The mean difference is around 50 % lower than the Pfeleiderer model and just half of the Stodola model's mean difference. The Qiu model's mean difference is comparable to the Wiesner model (10 % higher). For the RMSE, the results are comparable to the mean difference results. The Wiesner model is most suitable with a RMSE of 0.031. In contrast, the maximum difference is the lowest in the Pfeleiderer model (4.1 % lower than the Wiesner model). Overall, the Wiesner- and Qiu-model show the highest agreement to the CFD-data. The assessment is conducted with the absolute difference. Certainly, the authors also conducted an assessment on the relative difference and the overall outcome is equal. Nevertheless, small differences in the slip factor might have a huge relative impact on small slip velocities.

Table 2: Assessment of the absolute difference of the literature slip models to the CFD data

	Max	Mean	RMSE
Stodola	0.206	0.0412	0.0531
Pfeleiderer	0.165	0.0295	0.0382
Wiesner	0.172	0.0199	0.031
Qiu	0.185	0.0216	0.0348

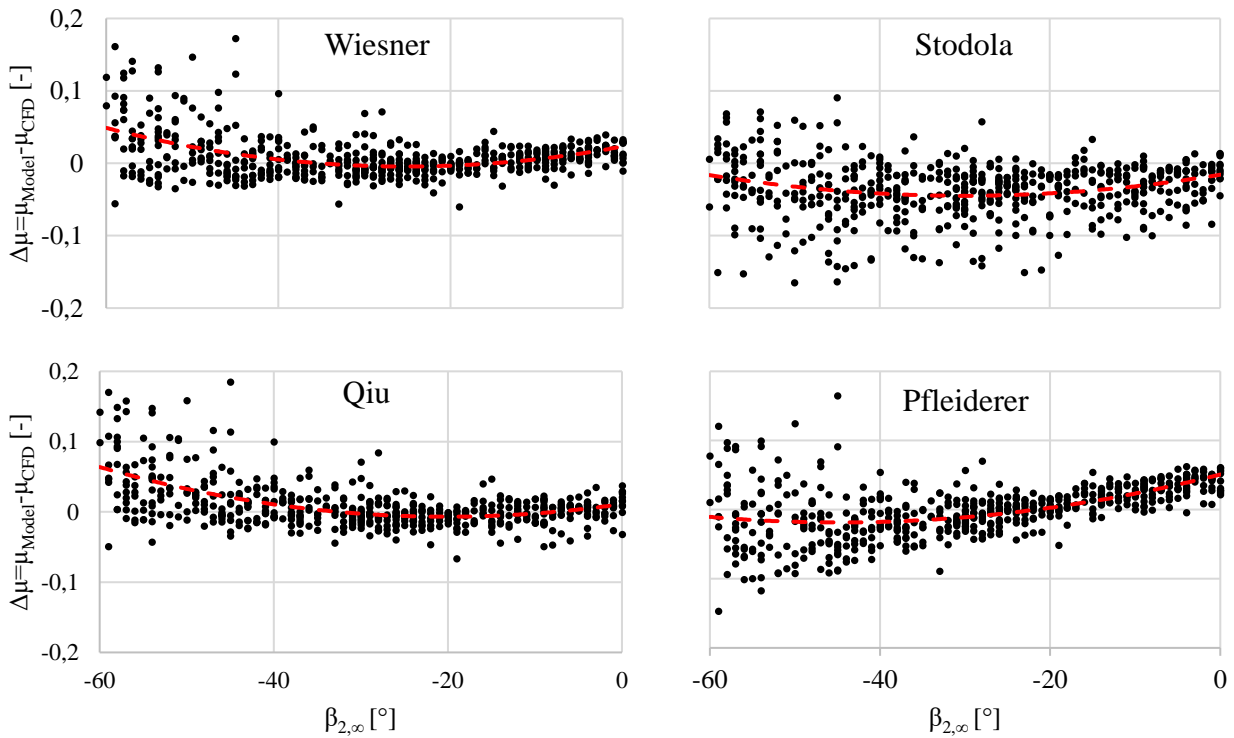


Figure 4: Visualization of the slip model difference of the four literature models to the CFD results for different blade outlet angles; Quadratic polynomial regression in red line

Besides the shown statistical analyses, the influence of the nine parameters on the slip model difference are determined. Therefore, the variation in slip model difference over the blade outlet angle is shown in figure 4. Overall, the results of the statistical analyses are underlined here. The scattering is comparably low for the Wiesner, Qiu and Pfeleiderer model. There are three main findings in this graphic: Firstly, especially for the Wiesner, Qiu and Pfeleiderer model the scattering depends on the

blade outlet angle. It increases with decreasing blade outlet angles. Secondly, the Pfeleiderer model has a negative gradient of modelling difference over the blade outlet angle. This underlines that the influence of blade outlet angle is overestimated in this model. Thirdly, the difference of the Qiu model compared to the difference of the Wiesner model is larger for blade outlet angles below -40° . As the scattering is significantly increasing for low outlet blade angles in the Wiesner, Qiu and Pfeleiderer model, a modelling error is indicated and therefore other parameter influences and flow phenomena might be linked to the slip modelling difference in this region.

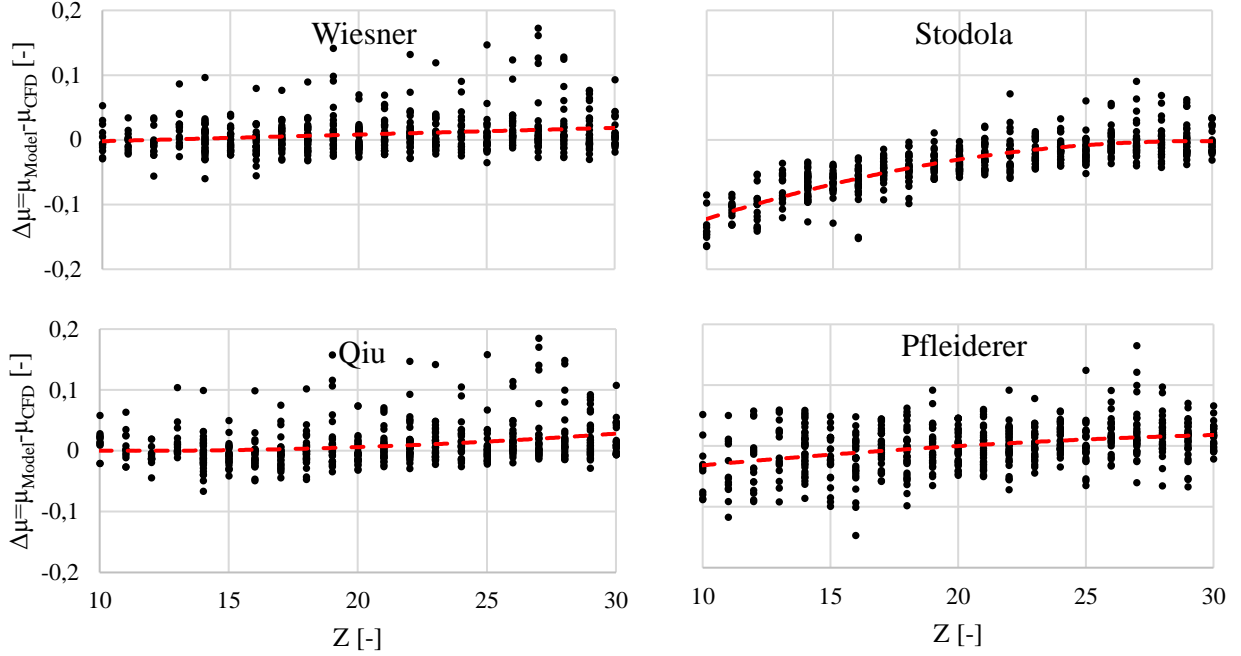


Figure 5: Visualization of the slip model difference of the four literature models to the CFD results for different blade numbers; Quadratic polynomial regression in red line

For the blade number variation, the difference between the literature slip models is larger (Figure 5). For all four models, a scattering with comparable amplitudes as for the blade outlet angle becomes apparent in figure 5. The polynomial regression line underlines an average fit of the blade number influence in CFD calculations and Wiesner model. For the Qiu model, the difference is slightly higher for high blade numbers. The other two models underestimate the influence for small blade numbers. The difference is the highest for the Stodola model but also detectable for the Pfeleiderer model. The visualization of figure 5 is in good agreement with the statistical results in table 2. Therefore, one reason for the good performance of the Wiesner model is the accurate modelling of blade number influence. When comparing the formulas 2 to 5, the blade number exponent in the Wiesner model (0.7) is differing from the exponents in the other models (1.0).

Furthermore, the influence of the specific speed n_s is analyzed in figure 6, as a huge influence is detected in the assessment. The specific speed gives a ratio of the rotational speed N , inlet volume flow rate Q_0 and specific compressor work y (equation 7, (Sigloch, 2006)). With the assumption of equivalent polytropic and isentropic efficiencies, the specific compressor work equals the isentropic enthalpy rise Δh_{is} .

$$n_s = \frac{N * \sqrt{Q_0}}{60 * y^{0.75}} * (2\pi^2)^{0.25} \cong \frac{N * \sqrt{Q_0}}{60 * \Delta h_{is}^{0.75}} * (2\pi^2)^{0.25} \quad (7)$$

Again, the scattering is the lowest for the Wiesner and Qiu model in figure 6. Moreover, a quadratic polynomial regression is created. For all four models, a dependency of the modelling difference on the specific speed is detectable. All models overestimate the slip factor with increasing specific speed. Besides the flow coefficient, the analyzed models do not contain a dependency on the operation conditions. Therefore, no information about the pressure rise or (isentropic) enthalpy change is included in the slip models and analyzed so far. In contrast, a huge influence of the specific speed and hence the isentropic enthalpy rise becomes apparent in figure 6. By integrating the specific speed into the models, an improvement of the slip models is expected by the authors.

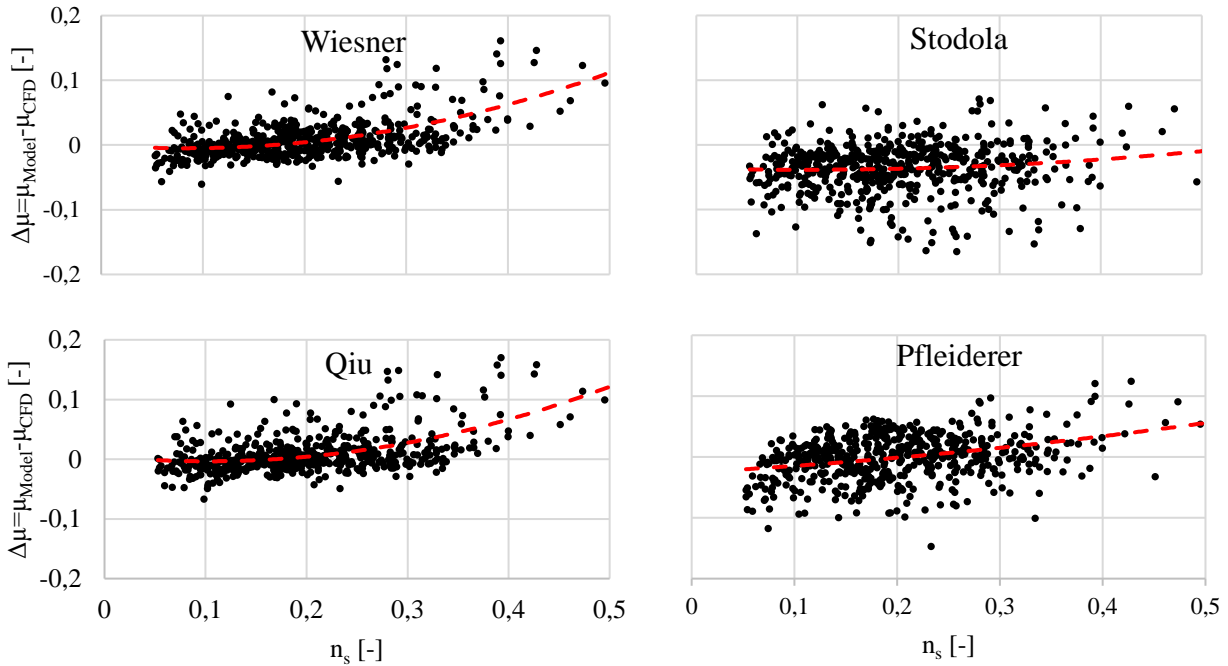


Figure 6: Visualization of the slip model difference of the four literature models to the CFD results for different specific speed numbers; Quadratic polynomial regression in red line

Finally, an analysis of variance (ANOVA) is conducted in ANSYS OptiSLang[®]. With the application of this analyzing method coupled with CFD, the impact of the different parameters on the compressor slip is estimated. Hence, the contributions of the different parameters on the total variance is determined. Due to parameter interdependencies and therefore mixed terms, the sum of contributions is above 100 %. (Dynardo, 2019)

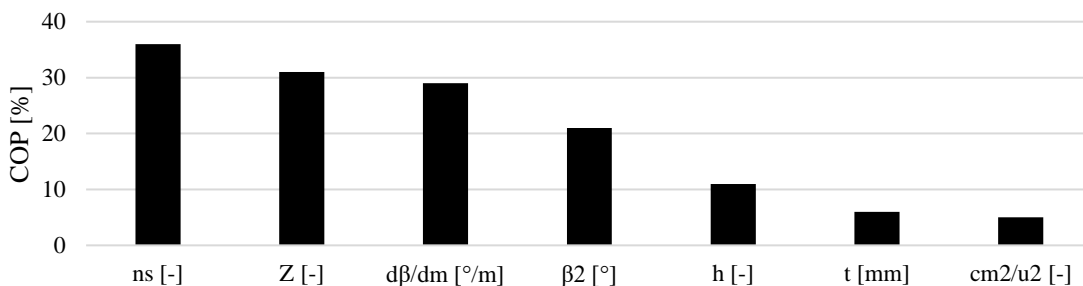


Figure 7: Results of the ANOVA for the CFD slip data

The results of the ANOVA are visualized in figure 7. For the analysis, all eleven parameters in table 1 are taken into account with the specific speed replacing the rotational speed and the flow coefficient replacing the mass flow. Also the intrinsic variation of blade outlet turning rate and pitch length are integrated. Based on the ANOVA, only seven parameters are necessary to describe the slip factor changes in the analyzed parameter ranges. The specific speed has the highest influence with a

COP of 36 %. The blade number, blade outlet turning rate and blade outlet angle have also comparable influence. The influence of the impeller tip gap, impeller thickness and flow coefficient is around or below a COP of 10 %. The analysis indicates that only two of the four main parameters are integrated in all four slip models.

CONCLUSIONS

In the first part of this paper, centrifugal compressor impeller geometries are varied with a DOE including 598 designs. For this database, slip factors are derived based on CFD analysis as well as well-known literature empirical models. In the second part, the results are compared by statistical evaluation in order to assess the accuracy of the empirical models. It is shown that the Wiesner model has the highest accuracy based on statistical values. The RMSE is 0.031 and therefore 12 % lower than the second best model (Qiu). In contrast, the maximum difference is the lowest in the Pfeleiderer model. Nevertheless, the analysis of dependency of modelling difference on the blade outlet angle and specific speed underlines the advantages of the Wiesner and Qiu model. An analysis of variance to find the influences of eleven parameters is conducted. With it, four parameters mainly influencing the compressor slip are detected. These are besides the blade number and blade outlet angle the specific speed as well as the blade outlet turning rate.

Besides the usage of the created data base for an assessment of consisting slip models, the data can be used for creation of a new CFD based slip model. The Wiesner model shows the highest accordance with the CFD data just integrating two of the four main influence parameters. Therefore, an integration of specific speed and blade turning rate in this model is promising. Furthermore, the shown assessment and ANOVA will assist this model creation process. The researchers are looking forward to introduce an own CFD based slip model. In addition, detailed flow analyses for different DOE impellers will help understanding the phenomena leading to compressor slip and slip modelling differences.

ACKNOWLEDGEMENTS

This research was partly funded by the Fraunhofer High-Performance Center DYNAFLEX[®] and the German State of North Rhine-Westphalia. The lead author would like to thank the Deutsche Bundesstiftung Umwelt DBU (German Federal Environmental Foundation) for funding his research.

REFERENCES

- Braembussche, R. V., (2019). *Design and Analysis of Centrifugal Compressors*. John Wiley & Sons, Ltd.
- Bräunling, W. J.G., (2009). *Flugzeugtriebwerke: Grundlagen, Aero-Thermodynamik, ideale und reale Kreisprozesse, Thermische Turbomaschinen, Komponenten, Emissionen und Systeme*. Springer Berlin, Heidelberg.
- Cumpsty, N., (1989). *Compressor Aerodynamics*. Longman Scientific & Technical.
- Cumpsty, N. A., Horlock, J. H., (2006). *Averaging Nonuniform Flow for a Purpose*. Journal of Turbomachinery. 128(1). 120-129.
- Dynardo, (2019). *Methods for multi-disciplinary optimization and robustness analysis*. 1-75.
- Eckardt, D., (1975). *Instantaneous Measurements in the Jet-Wake Discharge Flow of a Centrifugal Compressor Impeller*. Journal of engineering for power 97. 337-346.
- Eckardt, D., (1980). *Flow Field Analysis of Radial and Backswept Centrifugal Compressor Impellers - Part I: Flow Measurements Using a Laser Velocimeter*. International Gas Turbine Conference 25. 77-86.
- Eckert, B., Schnell, E., (1961). *Axial- und Radialkompressoren*. Springer Verlag Berlin Heidelberg.
- Guo, E.-M., Kim, K.-Y., (2004). *Three-Dimensional Flow Analysis and Improvement of Slip Factor Model for Forward-Curved Blades Centrifugal Fan*. KSME International Journal. 18(2). 302-312.

- Harrison, M. H., Key, N. L., (2020). *A New Approach to Modeling Slip and Work Input for Centrifugal Compressors*. Proceedings of ASME Turbo Expo, Virtual, Online.
- Huang, J.-M., Luo, K.-W., Chen, C.-F., Chiang, C.-P., Wu, T.-Y., Chen, C.-H., (2013). *Numerical Investigations of Slip Phenomena in Centrifugal Compressor Impellers*. International Journal of Jet-Engines. 30(1). 123-132.
- Kienzle, N., Waesker, M., di Mare, F., Buelten, B., Doetsch, C., (2019). *A Method For Matching Compressor Stage Characteristics To A Given Load Profile By Operating Point Weighting*. Proceedings of the 13th European Conference on Turbomachinery, Lausanne, Switzerland.
- Pfleiderer, C., Petermann, H., (1996). *Strömungsmaschinen*. Springer Verlag Berlin Heidelberg.
- Qiu, X., Jakipse, D., Zhao, J., Anderson, M., (2011). *Analysis and Validation of a Unified Slip Factor Model for Impellers at Design and Off-Design Conditions*. Journal of Turbomachinery. 133(4). 1-9.
- Roache, P. J., (1994). *Perspective: A Method for Uniform Reporting of Grid Refinement Studies*. Journal of Fluids Engineering. 116(3). 405–413.
- Schuster, P., Schmidt-Eisenlohr, U., (1980). *Flow Field Analysis of Radial and Backswept Centrifugal Compressor Impellers - Part II: Comparison of Potential Flow Calculations and Measurements*. International Gas Turbine Conference 25. 87-95.
- Sigloch, H., (2006). *Strömungsmaschinen – Grundlagen und Anwendungen*. Hanser Verlag. München.
- Stodola, A., (1924). *Dampf- und Gasturbinen*. Springer Verlag Berlin Heidelberg.
- Stuart, C., Spence, S., Filsinger, D., Starke, A., Kim, S., (2018). *A Three-Zone Modelling Approach For Centrifugal Compressor Slip Factor Prediction*. Proceedings of ASME Turbo Expo, Oslo, Norway.
- Waesker, M., Buelten, B., Kienzle, N., Doetsch, C., (2020). *Optimization of Supersonic Axial Turbine Blades Based On Surrogate Models*. Proceedings of ASME Turbo Expo, Virtual, Online.
- Wiesner, J. F., (1967). *A Review of Slip Factors for Centrifugal Impellers*. Journal of Engineering for Power. 89(4). 558-566.